

# Deacylated Pulmonary Surfactant Protein SP-C Transforms From $\alpha$ -Helical to Amyloid Fibril Structure via a pH-Dependent Mechanism: An Infrared Structural Investigation

Richard A. Dluhy,\* Saratchandra Shanmukh,\* J. Brian Leapard,\* Peter Krüger,\* and John E. Baatz<sup>†</sup>

\*Department of Chemistry, University of Georgia, Athens, Georgia; and <sup>†</sup>Medical University of South Carolina, Department of Pediatrics, Charleston, South Carolina

**ABSTRACT** Bovine pulmonary surfactant protein C (SP-C) is a hydrophobic,  $\alpha$ -helical membrane-associated lipoprotein in which cysteines C4 and C5 are acylated with palmitoyl chains. Recently, it has been found that the  $\alpha$ -helix form of SP-C is metastable, and under certain circumstances may transform from an  $\alpha$ -helix to a  $\beta$ -strand conformation that resembles amyloid fibrils. This transformation is accelerated when the protein is in its deacylated form (dSP-C). We have used infrared spectroscopy to study the structure of dSP-C in solution and at membrane interfaces. Our results show that dSP-C transforms from an  $\alpha$ -helical to a  $\beta$ -type amyloid fibril structure via a pH-dependent mechanism. In solution at low pH, dSP-C is  $\alpha$ -helical in nature, but converts to an amyloid fibril structure composed of short  $\beta$ -strands or  $\beta$ -hairpins at neutral pH. The  $\alpha$ -helix structure of dSP-C is fully recoverable from the amyloid  $\beta$ -structure when the pH is once again lowered. Attenuated total reflectance infrared spectroscopy of lipid-protein monomolecular films showed that the fibril  $\beta$ -form of dSP-C is not surface-associated at the air-water interface. In addition, the lipid-associated  $\alpha$ -helix form of dSP-C is only retained at the surface at low surface pressures and dissociates from the membrane at higher surface pressures. In situ polarization modulation infrared spectroscopy of protein and lipid-protein monolayers at the air-water interface confirmed that the residual dSP-C helix conformation observed in the attenuated total reflectance infrared spectra of transferred films is randomly or isotropically oriented before exclusion from the membrane interface. This work identifies pH as one of the mechanistic causes of amyloid fibril formation for dSP-C, and a possible contributor to the pathogenesis of pulmonary alveolar proteinosis.

## INTRODUCTION

Mammalian pulmonary surfactant is a highly specialized substance that contains ~85% phospholipid, 7–10% protein, and 4–8% neutral lipid (Creuwels et al., 1997; Notter, 2000). The most abundant phospholipid class is phosphocholine, whereas anionic phospholipids including phosphoglycerols make up ~10–15% of lung surfactant phospholipids (Hunt et al., 1991; Kahn et al., 1995; Holm et al., 1996). Lung surfactant also contains four apoproteins, including two small hydrophobic proteins, surfactant proteins B and C (SP-B and SP-C) that are known to enhance the adsorption and dynamic film behavior of phospholipids (Hawgood and Schiffer, 1991; Johansson et al., 1994a; Creuwels et al., 1997; Notter, 2000). The lack of surfactant in the underdeveloped lungs of premature infants is the root cause of neonatal respiratory distress syndrome (RDS) (Avery and Mead, 1959), while disruption of surfactant activity is linked to the pathophysiology of clinical lung damage seen in acute respiratory distress syndrome (ARDS) (Pison et al., 1989; Lewis and Jobe, 1993; Notter and Wang, 1997).

Mature bovine SP-C is secreted by type II epithelial cells into the alveoli in a complex mixture of surfactant lipids and proteins. Bovine SP-C consists of 34 amino acids and is an extremely hydrophobic, predominately  $\alpha$ -helical protein of ~4.0 kD with charged amino acids (K10 and R11) near its N-terminus. The cysteines C4 and C5 are acylated with C-16 (palmitoyl) chains in bovine SP-C. The NMR structure in apolar solvent describes the valine-, leucine-, and isoleucine-rich region of this small protein as a rigid rod in which only a few residues near the N-terminus (L1–P7) and the C-terminus are not helical (Johansson et al., 1994b). The length of this helix (V8–G34) is ~39 Å with a diameter of ~12 Å.

SP-C is associated with enhanced re-adsorption of phospholipids to the surfactant lipid monolayer at the air-water interface during monolayer expansion (the *in vitro* equivalent to inhalation) (Notter, 2000). It also appears to play a role in the formation of three-dimensional layers of surfactant during compression of the monolayer through a mechanism whereby SP-C assists in transfer of lipids from the monolayer to form stacked multilayer structures. Using *ex situ* microscopy methods, the SP-C-dependent formation of membrane-adherent particles has been demonstrated at high surface pressures (Amrein et al., 1997; von Nahmen et al., 1997; Kramer et al., 2000), and a model for the formation of multibilayer phospholipid reservoirs, stabilized by SP-C, has been proposed (Galla et al., 1998; Kramer et al., 2000). Research from this laboratory has demonstrated that SP-C also catalyzes the formation of micrometer-sized, surface-associated, three-dimensional particles at the interface, as visualized using scattered light dark-field micros-

Submitted June 9, 2003, and accepted for publication June 23, 2003.

Address reprint requests to Richard A. Dluhy, Dept. of Chemistry, University of Georgia, Athens, GA 30602-2556. Tel.: 706-542-1950; Fax: 706-542-9454; E-mail: dluhy@chem.uga.edu.

Peter Krüger's present address is University of Leipzig, Inst. of Experimental Physics I, Linnéstrasse 5, D-04103 Leipzig, Germany.

© 2003 by the Biophysical Society

0006-3495/03/10/2417/13 \$2.00

copy with grazing incidence laser illumination (Krüger et al., 1999, 2002).

These microscopy studies have been complemented by IR spectroscopic studies at the air-water interface that are able to study the secondary structure of proteins in monolayers and thin films (Mendelsohn et al., 1995; Dluhy, 2000). External reflectance IR has the sensitivity required to observe the amide I vibration of the SP-C protein in pure or highly enriched lipid-protein films and obtain protein structural information. This reflection IR technique has been applied to the study of monolayer films of extracted lung preparations (Dluhy et al., 1989) and more recently, to investigate the structure-function relationships of the lung surfactant proteins SP-B and SP-C in lipid monolayers (Pastrana-Rios et al., 1995; Gericke et al., 1997; Flach et al., 1999; Bi et al., 2002; Brockman et al., 2002; Shanmukh et al., 2002).

These previous IR studies have confirmed the predominantly  $\alpha$ -helical nature of fully acylated SP-C at the air-water interface, and showed how this structural motif is optimized to interact with the monolayer phospholipids. Lately, however, a different picture has emerged that suggests that the  $\alpha$ -helix is not the final, stable structure previously described for SP-C, and that other structural intermediates are available to the SP-C molecule. For example, under certain conditions, SP-C has been shown to transform from a monomeric  $\alpha$ -helix to an aggregated  $\beta$ -sheet conformation (Szyperski et al., 1998). This  $\alpha \rightarrow \beta$  conversion results in protein aggregates that visually resemble amyloid fibrils (Gustafsson et al., 1999). It has previously been reported that amyloid fibrils composed of SP-C occur in pulmonary alveolar proteinosis (PAP), a disease in which lipid-protein aggregates accumulate in the alveoli (Seymour and Presneill, 2002). In particular, the deacylation of SP-C has been shown to increase the rate of peptide aggregation and fibril formation, presumably by destabilization of the  $\alpha$ -helix with a concomitant increase in  $\beta$ -aggregation (Gustafsson et al., 2001). These studies suggest that  $\alpha$ -helical SP-C is actually a metastable intermediate that may convert to  $\beta$ -aggregate and fibril forms, depending upon the kinetics of the particular pathways available and the milieu in which it resides. Unfortunately, the specific pathways and causes of amyloid fibril formation for proteins in general, and SP-C in particular, are not well understood (Kallberg et al., 2001).

In contrast to the fully acylated form of SP-C, which IR spectroscopy studies have uniformly shown to be  $\alpha$ -helical, the previously published IR spectra of deacylated SP-C (dSP-C) show no consistent trend. In a mixed organic solvent, dSP-C was shown to fully transform from a monomeric  $\alpha$ -helix to aggregated  $\beta$ -sheet (Szyperski et al., 1998). Other studies of dSP-C associated with lipids report that after nucleophilic cleavage of the palmitoyl groups, the  $\alpha$ -helical content of dSP-C decreased (and the  $\beta$ -strand content increased), but the protein still retained significantly helical content (Vandenbussche et al., 1992; Wang et al., 1996). In contrast, an IR external reflection study of dSP-C at

the air-water (A/W) interface showed that deacylation did not alter the protein secondary structure (Flach et al., 1999).

In the current work we report that deacylated SP-C exhibits a reversible pH-dependent conformational change from an  $\alpha$ -helical to an extended  $\beta$ -strand amyloid fibril-like conformation. Multiple IR spectroscopic techniques were employed to assess the secondary structure of dSP-C in solution, bulk liposomes, lipid-protein films, and in lipid-protein monolayers at the A/W interface. IR methods used in this study include transmission IR spectroscopy of solutions and bulk liposomes, attenuated total reflectance (ATR) spectroscopy of transferred thin films, and photoelastic modulation IR external reflection spectroscopy (PM-IRRAS) of monolayers at the A/W interface. This work identifies pH as one of the mechanistic causes of amyloid fibril formation for dSP-C, and a possible contributor to the pathogenesis of pulmonary alveolar proteinosis.

## MATERIALS AND METHODS

### Surface chemistry

The synthetic phospholipids 1,2-dipalmitoyl-*sn*-glycero-3-phosphoglycerol (DPPC) and 1,2-dipalmitoyl-*sn*-glycero-3-phosphoglycerol (DPPG) were purchased from Avanti Polar Lipids (Alabaster, AL) and used as received. ACS grade NaCl and HPLC grade methanol and chloroform were obtained from J.T. Baker, (Phillipsburg, NJ). Ultrapure H<sub>2</sub>O was obtained from a Barnstead (Dubuque, IA) ROPure/Nanopure reverse osmosis/deionization system and had a nominal resistivity of 18.3 M $\Omega$  cm. The subphase used in these experiments was 120 mM NaCl, adjusted to pH 7 with a phosphate buffer.

### Purification of surfactant protein C (SP-C)

SP-C was purified from calf lung surfactant extract (CLSE) by isocratic normal phase liquid chromatography on Silica C8 as described elsewhere (Baatz et al., 2001). Briefly, ~700 mg CLSE (total lipid plus protein) was initially reduced in volume by evaporation under nitrogen to ~4 ml (~1% of column bed volume). Small amounts of chloroform were added to the concentrated CLSE if the solution became cloudy. The concentrated CLSE was then applied to a 450-ml bed volume LC column that had been pre-equilibrated with 7:1:0.4 MeOH/CHCl<sub>3</sub>/5% 0.1 N HCl. The added CLSE was allowed to completely adsorb to the column, and was then eluted with 7:1:0.4 MeOH/CHCl<sub>3</sub>/5% 0.1 N HCl at a flow rate of 0.4 ml/min and UV detection at 254 nm. SP-C eluted from the column as the second peak as determined by SDS PAGE and protein sequencing (see below). Fractions containing SP-C were combined, concentrated via N<sub>2</sub> gas stream and run on a second C8 LC column. Fractions containing purified SP-C from this second column were combined and concentrated by N<sub>2</sub> gas stream. Purified SP-C was then dialyzed against CHCl<sub>3</sub>:MeOH (7:1) + 5.0% 0.1 N HCl. Phospholipid content of purified SP-C using the method of Shin (1962) was determined to be <4 mol lipid/mole SP-C. Protein sequencing analysis (see below) indicated that the purified SP-C was free of SP-B.

### SDS PAGE and amino acid analysis

For SDS PAGE, 20  $\mu$ L of the appropriate column fractions were dried, resuspended in NuPage sample buffer (Invitrogen, Carlsbad, CA) and applied to 4–10% gradient acrylamide Tris/Bis gels (NuPage gels,

Invitrogen) under nonreducing conditions. Electrophoresis was performed at a constant voltage of 200 V for 40 min with a morpholinoethanesulphonic acid buffer containing 50 mM morpholinoethanesulphonic acid/50 mM Tris base/3.5 mM SDS/1 mM EDTA, pH 7.7 as the running buffer. Silver staining for detection of protein bands was performed according to Morrissey (1981). N-terminal amino acid sequence analysis was performed for 7–10 cycles using an Applied Biosystem Procise sequence analyzer (Applied Biosystem, Foster City, CA). SP-C was identified by the N-terminal sequences of Leu-Ile-Pro-???-???-Pro-Val, where positions 4 and 5 in the SP-C sequence were both assumed to be Cys. The concentration of SP-C in solution was determined by the BCA total protein assay (Sigma Chemical, St. Louis, MO).

## Deacylation of SP-C

Deacylation of SP-C was achieved by acid hydrolysis of the SP-C thioester groups. Hydrolysis was carried out by incubation of SP-C in a solution of 7:1 methanol/chloroform + 5% 0.1 N HCl at 20°C for 72 days. Mass spectrometry, as described below, was used to verify deacylation of the SP-C.

## Mass spectrometry

Mass spectral data was obtained on a Bruker Reflex time-of-flight (TOF) instrument (Bruker Instruments, Billerica, MA) using matrix assisted laser desorption ionization (MALDI) in the Chemical/Biological Mass Spectrometry Facility at the University of Georgia. Protein samples were mixed with sinapinic acid in H<sub>2</sub>O:CH<sub>3</sub>CN:TFA and spotted onto a MALDI plate and allowed to dry. The dried sample plates were introduced into the spectrometer under high vacuum where a pulsed nitrogen laser (337-nm wavelength) is used to desorb and ionize the sample. The instrument was run in reflector (electrostatic mirror) mode to spatially collimate the ion beam and produce time/energy focusing. The sample was ionized using ~120 pulses from the N<sub>2</sub> laser and a 10- $\mu$ s delay. After the >3 meter flight tube, ions were detected using ultra-fast dual microchannel plates. Mass accuracy for this instrument is ~4 m/z units.

## Preparation of samples

Stock lipid solutions of DPPC and DPPG (~2.5 mg/ml) were prepared in 4:1 CHCl<sub>3</sub>:MeOH. Solutions of the lipid and proteins containing DPPC, DPPG and dSP-C were prepared by mixing the appropriate amounts of the phospholipid stock solution together with the stock solutions of dSP-C in 1:1 CHCl<sub>3</sub>:MeOH.

## Transmission IR experiments

To follow the structure of dSP-C with increasing pH, an aliquot (150  $\mu$ L) of the dSP-C stock solution was obtained having an initial pH of 1.8. This sample was progressively neutralized with 0.01 N NaOH. This low concentration of NaOH was chosen so as to finely adjust the pH of the stock solution. The pH of the protein solutions was measured using a 12-cm-long Glass Micro-pH combination electrode (Thermo-Orion), connected to a Beckman Phi 40 pH meter (Beckman, Fullerton, CA). The electrode was standardized using pH = 4.0 and pH = 7.0 buffer solutions.

At different pH values during the neutralization process, 10  $\mu$ L aliquots of the sample solution were withdrawn and deposited on a CaF<sub>2</sub> crystal. After the evaporation of the solvent, transmission IR spectra of the samples were collected using a PerkinElmer 2000 (Norwalk, CT) FT IR spectrometer equipped with a DTGS detector. Spectra were recorded using 100 scans at 8 cm<sup>-1</sup> resolution with triangular apodization and one level of zero filling. The transmission IR spectra were baseline-corrected using the Grams/AI spectral software package (Ver. 6.0, Galactic Industries, Salem, NH). Otherwise, the spectra have not been smoothed or further processed.

To illustrate the reversibility of the structure of dSP-C with decreasing pH, the stock solution of dSP-C (initial pH of 1.8) was neutralized using 0.1 N NaOH to a pH of 8.7. The pH of the solution was then reduced using 0.01 N HCl. At different points as the solution decreased in pH, a 10- $\mu$ L aliquot of the sample was withdrawn and placed on CaF<sub>2</sub> windows. After evaporation of the solvent, transmission IR spectra of these aliquots were obtained using the parameters described above.

## Langmuir-Blodgett monolayer transfers

Lipid-protein monolayers were deposited onto monocrystalline, trapezoidal germanium (Ge) attenuated total reflectance (ATR) elements. The Ge ATR elements (Spectral Systems, Hopewell Junction, NY) had dimensions of 50 × 10 × 2 mm with 45° face angles, and a total surface area of 12.6 cm<sup>2</sup>. Ge crystals were cleaned before Langmuir-Blodgett (L-B) film deposition by sonication for 15 min in a 6:4:1 chloroform:methanol:water solution, followed by sonication twice for 15 min each in ultrapure water.

Monomolecular films were transferred onto the Ge ATR crystals using a fully programmable Joyce-Loebl Ltd. (Gateshead, England) Langmuir-Blodgett trough equipped with a constant-perimeter PTFE-coated fiberglass tape to control the size of the trough area. The subphase temperature was held constant to 21 ± 1°C by flowing thermostated water through the hollow body of the PTFE coated aluminum trough. Surface pressure measurements were recorded by differential weight measurements with a filter paper (Whatman No. 1) Wilhelmy plate suspended from a microbalance. The surface of the L-B trough was determined to be clean if the surface pressure did not increase by more than 0.2 mN/m while compressing to minimum area at full speed.

To prepare a transfer, a Ge crystal was fully immersed into the subphase through a clean surface. The lipid-protein sample was applied to the trough surface via a microsyringe and allowed to equilibrate for 15 min. The monolayer was compressed at 5.5 cm<sup>2</sup>/min to the final surface pressure (e.g., 30, 45, or 60 mN/m). The Ge crystal was vertically raised from the subphase through the monolayer film at a linear rate of 4 mm/min while the surface pressure was held constant to ± 1.0 mN/m. Transfer ratios were calculated for each sample and were always between 0.9 and 1.1.

## Attenuated total reflectance IR experiments

Attenuated total reflectance infrared spectra were acquired using a BioRad/Digilab (Cambridge, MA) FTS-40 spectrometer equipped with a narrow band, LN<sub>2</sub>-cooled HgCdTe detector. Spectra were recorded with 1024 co-added scans at 4 cm<sup>-1</sup> resolution using triangular apodization and one level of zero filling. The Ge ATR crystal was mounted into a horizontal ATR accessory (CIC Photonics, Albuquerque, NM); the system was purged with dry air for 15 min before data collection. ATR spectra were acquired using a background spectrum of the Ge crystal at room temperature just before L-B film deposition. ATR-IR spectra were baseline-corrected using the Grams/AI spectral software package. Otherwise, the spectra have not been smoothed or further processed. Vibrational band heights, wavenumber peak positions, and integrated intensities were calculated using a 5-point center-of-gravity algorithm (Cameron et al., 1982), written in our laboratory for the Grams environment.

## Polarization modulation-IRRAS measurements

Polarization-modulation IR reflection-absorption (PM-IRRAS) measurements at the A/W interface were performed using a Bruker Instruments Equinox 55 Fourier transform infrared spectrometer optically interfaced to a variable angle external reflection accessory (Bruker model XA511-A). The external reflection accessory was equipped with a custom-designed Langmuir trough (Riegler and Kirstein, Berlin, Germany) containing a microbalance Wilhelmy sensor for surface pressure readings. PM-IRRAS

measurements were performed using previously described protocols (Blaudez et al., 1993; Buffeteau et al., 1993; Blaudez et al., 1996; Buffeteau and Pezolet, 1996), with changes adapted for our particular experimental design. The IR beam from the interferometer was directed through its external beam port and steered using mirrors into the excitation arm of the reflectance accessory. This IR beam is singly modulated at frequencies  $f = 2V\tilde{\nu}$ , where  $V$  is the scan speed of the interferometer and  $\tilde{\nu}$  is the wavenumber of the IR radiation, resulting in a spectral bandwidth of  $\sim 0.4\text{--}6.5$  kHz.

The excitation arm of the external reflection accessory was rotated using computer-driven stepper motors to achieve an angle of incidence of  $74^\circ$ . Before reflection from the A/W interface, a wire-grid polarizer (IGP225, Moletron Detector, Portland, OR) passed  $p$ -polarized light through a ZnSe photoelastic modulator (PEM-90, Hinds Instruments, Hillsboro, OR) operating at its resonance frequency  $f_m$  of 50 kHz. The application of a sinusoidal input voltage to the PEM crystal induced a linear modulation of the IR beam between  $p$ - and  $s$ -polarization states at a  $2f_m$  frequency of 100 kHz, resulting in a second, high frequency modulation of the IR radiation. After reflection from the A/W interface, the doubly modulated IR radiation was collected by an  $f/1$  ZnSe lens and focused onto the  $1\text{-mm}^2$  sensing chip of a liquid  $N_2$ -cooled photovoltaic HgCdTe detector (KMPV11, Kolmar Technologies, Newburyport, MA).

Due to the fact that the spectral frequencies from the interferometer are more than an order of magnitude removed from the modulation frequencies added by the PEM, the signal from the HgCdTe detector preamplifier may be separated into sum ( $I_{dc}$ ; resulting from the IR spectrometer) and difference ( $I_{ac}$ ; resulting from PEM modulation) components using dual-channel electronics with lock-in detection, as previously described (Blaudez et al., 1993; Buffeteau and Pezolet, 1996). The  $I_{ac}$  difference signal was demodulated at  $2f_m$  with a digital lock-in amplifier (Stanford Research Systems, Model SR830) using a  $100\text{-}\mu\text{s}$  time constant. The  $I_{ac}$  difference signal from the output of the lock-in, as well as the  $I_{dc}$  sum signal, was filtered using low-pass filters; electronic filtering was achieved using dual-channel electronics (Stanford Research System, Model SR650). At the output of the electronic filters, both  $I_{ac}$  and  $I_{dc}$  signals were combined using a multiplexer and sent to the 16-bit ADC of the Bruker IR spectrometer. The combined signal was deconstructed and Fourier-transformed using spectrometer software. The ratio of the resulting  $I_{ac}$  and  $I_{dc}$  single beam spectra provides the PM-IRRAS signal  $S$  (Blaudez et al., 1993):

$$S = \frac{I_{ac}}{I_{dc}} = C \frac{J_2(\phi)(R_p - R_s)}{(R_p + R_s) + J_0(\phi)(R_p - R_s)}$$

In this equation,  $C$  is a constant that is the ratio of the slightly different electronic amplification of the two signal channels, and  $J_n(\phi_0)$  is the  $n^{\text{th}}$ -order Bessel function of maximum dephasing  $\phi_0$  introduced by the PEM. In our case, the PEM was set to introduce maximum dephasing ( $\phi_0 = \pi$ ) at  $2000\text{ cm}^{-1}$ . The PM-IRRAS spectra shown here are presented as normalized difference spectra, where  $\Delta S$  reflects the difference in signal intensity between the film-covered surface ( $S$ ) and the bare water surface ( $S_0$ ):

$$\Delta S = \frac{S - S_0}{S_0}$$

PM-IRRAS spectra were recorded at a resolution of  $4\text{ cm}^{-1}$  using a scan speed/sampling frequency of 13 kHz. The total acquisition time for each spectrum was 20 min, resulting in 800 interferograms per spectrum.

## RESULTS AND DISCUSSION

### Mass spectrometry of dSP-C

Fig. 1 presents the MALDI-TOF spectrum of the deacylated SP-C protein after acidic hydrolysis of the thioester-linked palmitoyl groups at cysteines C4 and C5. Bovine SP-C in its fully acylated form has an expected molecular mass of 4058

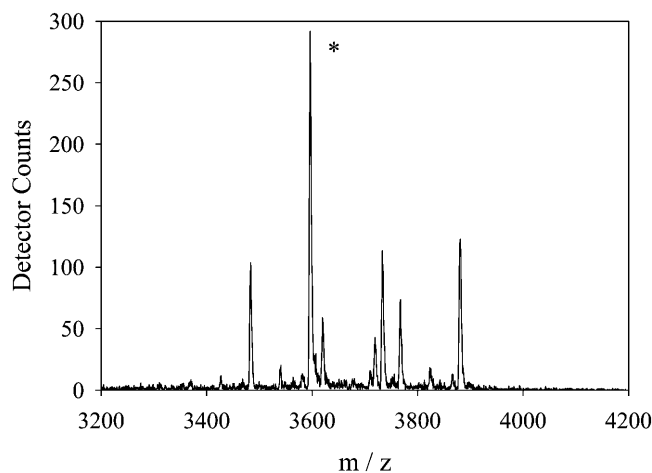


FIGURE 1 MALDI-TOF mass spectrum of deacylated SP-C. The major peak in the spectrum at 3596  $m/z$  (labeled with *asterisk*) represents the mass of the completely deacylated SP-C protein minus both palmitoyl chains. There is no peak present at 4058 Da, which corresponds to the mass of native, diacylated bovine SP-C, indicating acid hydrolysis of SP-C thioester groups was complete.

Da. This particular mass is absent from the mass spectrum of dSP-C shown in Fig. 1 indicating that little, if any, fully acylated SP-C exists in the sample. The major peak at 3596  $m/z$  in the mass spectrum of dSP-C (labeled with an *asterisk* in Fig. 1) corresponds to the mass of the fully acylated SP-C protein minus both covalently linked palmitoyl chains. The  $Na^{2+}$  adduct of this base peak also occurs at the expected value of 3620  $m/z$ . A truncated form of the polypeptide appears at 3483  $m/z$  indicating the loss of the N-terminal leucine from the amino acid chain. The peak at 3880  $m/z$  is the intact (nontruncated) monopalmitoylated form of the protein. The N-terminus truncated, one-chain peptide and its  $Na^{2+}$  adduct are observed at 3719  $m/z$  and 3733  $m/z$ , respectively. The mass peaks shown in Fig. 1 demonstrate the successful acidic hydrolysis of the acyl chains of SP-C.

### Visible microscopy of dSP-C amyloid fibrils

Using visible light microscopy, we have observed the formation of amyloid fibrils from solutions of deacylated bovine SP-C (dSP-C). Approximately  $150\text{ }\mu\text{L}$  of the stock solution of dSP-C in 7:1 methanol/chloroform + 5% 0.1 N HCl was pipetted onto a clean glass microscope slide. The solvent was permitted to partially evaporate before image acquisition. Images were obtained using an Olympus BX41 microscope at  $40\times$  magnification, fitted with an Olympus DP11 digital camera. Fig. 2 shows the image of the fibrils formed from the dSP-C solution. The image of the fibrils presented in Fig. 2 are consistent with previously published images of amyloid fibrils of deacylated SP-C isolated from the bronchoalveolar lavage of a clinical patient suffering from pulmonary alveolar proteinosis (PAP) (Gustafsson et al., 1999).

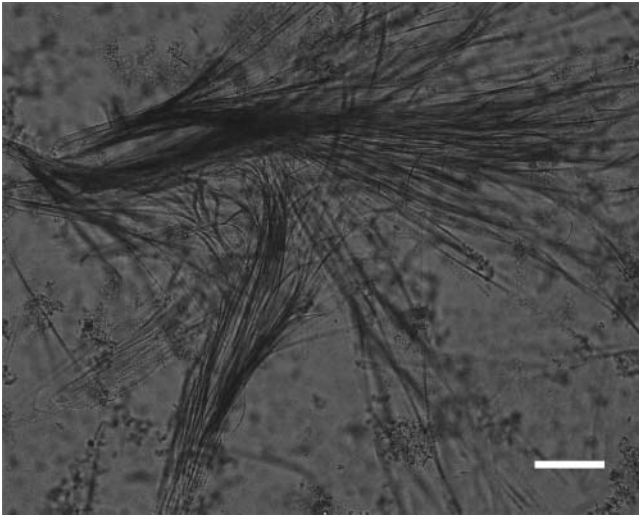


FIGURE 2 Amyloidlike aggregates of deacylated bovine SP-C (dSP-C) detected by visible light microscopy, 40 $\times$  magnification. Approximately 150  $\mu$ L dSP-C in 7:1 methanol/chloroform + 5% 0.1N HCl was pipetted onto a clean glass microscope slide. Solvent was permitted to partially evaporate before image acquisition using an Olympus DP11 digital camera coupled to an Olympus BX41 microscope. The bar in the figure represents a distance of 10  $\mu$ m.

### The pH dependence of dSP-C secondary structure in solution

Fig. 3 illustrates the amide I region (1720–1580  $\text{cm}^{-1}$ ) of dSP-C solutions obtained by transmission IR spectroscopy. These spectra were obtained by pH titration of the stock dSP-C solution (7:1 MeOH:CHCl<sub>3</sub> + 5% 0.1N HCl) with 0.01 N NaOH. A number of 10- $\mu$ L aliquots were removed from the titrated solution at the pH values indicated on the figure. The aliquots were deposited on CaF<sub>2</sub> windows and the solvent was allowed to evaporate before data collection.

The transmission IR spectra of dSP-C shown in Fig. 3 are presented as a function of increasing pH, beginning with the acidic pH samples at the bottom of the figure. The spectra of dSP-C at pH 1.8 shows two main peaks for the protein amide vibration, one at 1656  $\text{cm}^{-1}$  and one at 1626  $\text{cm}^{-1}$ . These two vibrations have been previously observed in the IR spectra of fully acylated SP-C at the A/W interface (Shanmukh et al., 2002). The wavenumber values of these amide I bands may be associated with specific protein secondary structure conformations using previously published IR spectra-structure correlations (Jackson and Mantsch, 1993; Goormaghtigh et al., 1994). The band at 1656  $\text{cm}^{-1}$  in the spectrum of SP-C is most commonly associated with this protein's  $\alpha$ -helical secondary structure (Pastrana-Rios et al., 1995). However, the band at 1626  $\text{cm}^{-1}$  is not commonly identified with a specific protein conformation. Rather, it is assigned to a structure of extended, multistrand aggregates (Kubelka and Keiderling, 2001b). The 1626  $\text{cm}^{-1}$  vibration has also been previously observed in the IR spectra of fully acylated SP-C,

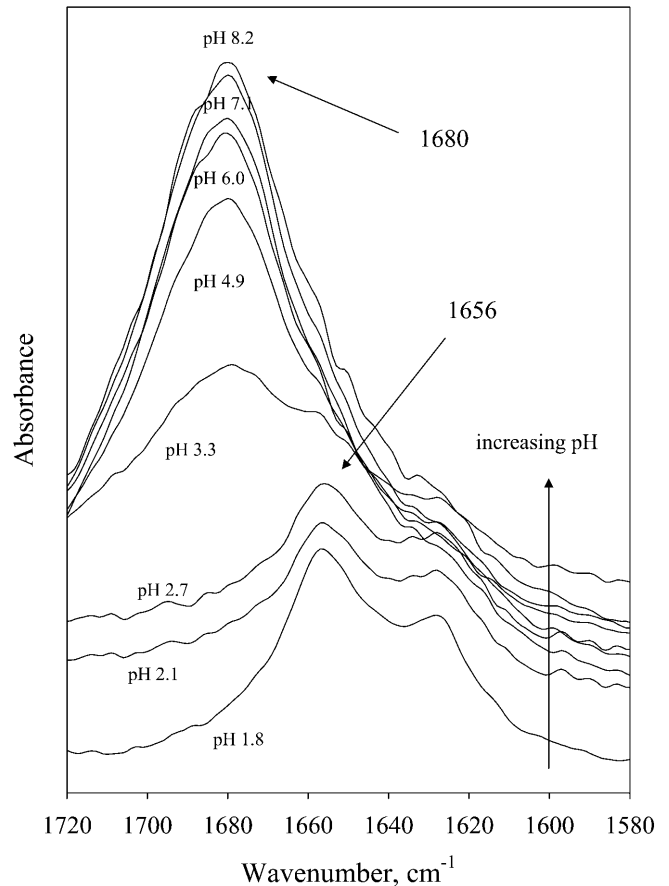


FIGURE 3 Transmission IR spectra of dSP-C in the amide I spectral region. Samples were prepared by titration of stock dSP-C solution (dissolved in 7:1 MeOH:CHCl<sub>3</sub> + 5% 0.1 N HCl) with 0.01 N NaOH. Aliquots were obtained at the pH values indicated in the figure and placed on CaF<sub>2</sub> disks. Spectra were obtained after solvent evaporation.

and has been attributed to protein aggregation in these samples (Pastrana-Rios et al., 1995; Shanmukh et al., 2002). The spectra of dSP-C presented here suggest that the deacylated protein at low pH adopts a primarily  $\alpha$ -helical secondary structure similar to that of the fully acylated protein at neutral pH.

As seen in Fig. 3, the IR spectra of dSP-C change markedly as the pH of the solution is increased. Between pH values of 2.7 and 3.3, the  $\alpha$ -helical band at 1656  $\text{cm}^{-1}$  as well as the aggregation band at 1626  $\text{cm}^{-1}$  band gradually decrease in intensity whereas a new band at  $\sim$ 1680  $\text{cm}^{-1}$  grows in intensity, finally becoming predominant at pH values  $>$ 4.9.

The commonly accepted interpretation of  $\beta$ -sheet structure in IR spectroscopy features a characteristically split spectral signature: a prominent band at  $\sim$ 1630  $\text{cm}^{-1}$  and a smaller feature at higher wavenumber,  $\sim$ 1680–1690  $\text{cm}^{-1}$  (Krimm and Bandekar, 1986). This split IR pattern for  $\beta$ -sheet proteins is usually attributed to aggregated strands stabilized by intermolecular hydrogen bonds (Jackson and Mantsch, 1993); however, this particular split amide I band

profile may only be characteristic for large extended antiparallel  $\beta$ -sheet structures (Harris, 2000). Recent research has indicated that a different IR spectral pattern may exist for smaller peptides containing short twisted  $\beta$ -sheet strands or  $\beta$ -hairpins (Silva et al., 2000). In addition, *ab initio* calculations for short model  $\beta$ -sheet peptide strands reveal that coiled or twisted forms of  $\beta$ -structures have much less amide I splitting than is observed in multi-kDa proteins containing aggregated, extended  $\beta$ -strands (Kubelka and Keiderling, 2001a,b).

The main amide I band observed at  $1680\text{ cm}^{-1}$  in the pH-dependent IR spectra at greater than pH 4 (Fig. 3) does not correlate with the classical picture of an extended, antiparallel  $\beta$ -sheet. Rather, a primary amide I vibration at  $1680\text{ cm}^{-1}$  is consistent with short segments of twisted or coiled  $\beta$ -sheet strands or  $\beta$ -hairpins in the amyloid fibril structure of dSP-C that have not aggregated into a supramolecular structure. In support of this interpretation, computer simulations of coiled or twisted  $\beta$ -strands predict that a single intense amide I band should occur at a higher wavenumber value than that of a regular planar  $\beta$ -sheet (Kubelka and Keiderling, 2001b). (Note, however, that due to the constraints of the computational methods, the wavenumber values resulting from the *ab initio* calculations are not directly comparable to the experimentally determined wavenumbers.) Other IR studies of  $\beta$ -amyloid proteins have also documented the presence of an amide I vibration at  $\sim 1680\text{ cm}^{-1}$ , including the lipid association of amyloid- $\beta$  protein from brain (Koppaka and Axelsen, 2000) and an early study of deacylated SP-C (Szyperski et al., 1998). In both these studies, however, a strong amide I vibration also occurs at  $\sim 1620\text{ cm}^{-1}$ , indicating that extensive protein aggregation has occurred in these samples.

Fig. 4 illustrates the extent to which each dSP-C conformation contributes to the overall band profile as a function of pH. This figure was generated by first curve-fitting the pH-dependent transmission spectra from Fig. 3. Three bands were used for the curve fitting, one at  $1680\text{ cm}^{-1}$  ( $\beta$ -amyloid conformation), one at  $1656\text{ cm}^{-1}$  ( $\alpha$ -helix), and one at  $1625\text{ cm}^{-1}$  (protein aggregation). In the curve-fitting procedure, the frequencies of the bands were fixed while the bandwidths were allowed to vary. The integrated intensities of each curve-fit band were then used to calculate the percentage of the amide I band area attributable to each conformation. It is clear from the curve-fitting results in Fig. 4 that the  $\beta$ -amyloid band at  $1680\text{ cm}^{-1}$  is the major contributor to protein structure above pH 3, with  $\sim 55\%$  of the amide I intensity centered in that band. However, the residual  $\alpha$ -helix and aggregation peaks are still present in substantial amounts at neutral pH, contributing  $\sim 30\%$  and  $10\%$ , respectively, to the overall amide I band intensity.

We have also investigated the reversibility of the helix-to-amyloid dSP-C conformational transition. Beginning with the dSP-C solution at low pH (1.8), the pH of sample was gradually neutralized by titration with 0.01 N NaOH, as

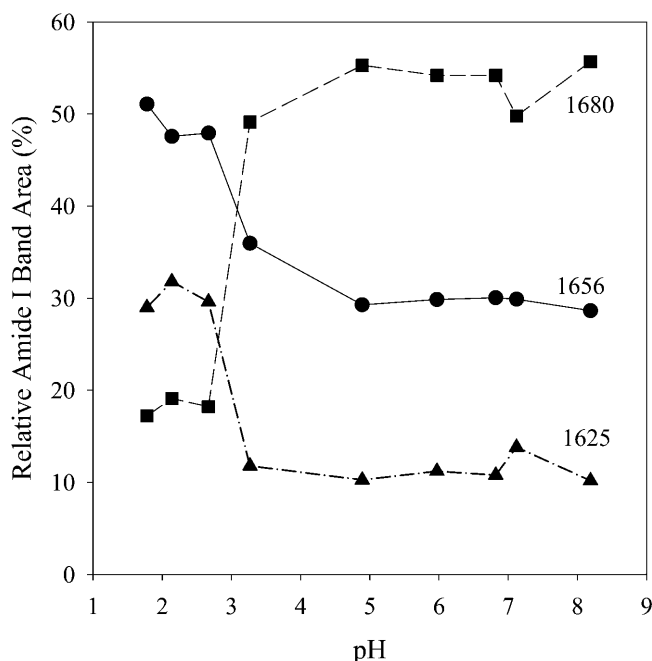


FIGURE 4 Percent of the entire amide I band intensity attributable to the major IR bands observed in the transmission IR spectra of dSP-C (Fig. 3) plotted as a function of pH. Peaks at  $1680\text{ cm}^{-1}$  correspond to amyloid  $\beta$ -structure,  $1656\text{ cm}^{-1}$  to  $\alpha$ -helix, and  $1626\text{ cm}^{-1}$  to aggregated protein.

described above and as seen in Fig. 3. The pH of the sample was then lowered by titration with 0.01 N HCl. In this case, aliquots of the sample solution were removed for IR analysis at specific pH values as the pH was lowered. Fig. 5 illustrates the effect of reversing the sample pH on peptide conformation. The upper spectrum (Fig. 5 A) was obtained at pH 4.5 and shows a broad amide I band with a main peak at  $1679\text{ cm}^{-1}$  along with a shoulder at  $1656\text{ cm}^{-1}$ . The presence of these two bands indicates that as the pH is being lowered, the  $\alpha$ -helix conformation begins to re-emerge alongside the amyloid  $\beta$ -structure. The lower spectrum (Fig. 5 B) demonstrates that when the pH is lowered to 1.5, the  $\alpha$ -helix is the only conformation present for dSP-C. These spectra illustrate that the  $\alpha$ -helix structure of dSP-C is fully recoverable from the amyloid  $\beta$ -type structure, and that a pH-dependent mechanism is responsible for the transition between the two forms.

The structure of dSP-C in the presence of lipids was further investigated by transmission IR spectroscopy. For these samples, stock lipid solutions of DPPC and DPPG ( $\sim 2.5\text{ mg/ml}$  in  $\text{CHCl}_3:\text{MeOH}$ ) were prepared. An organic solution containing 7:3 DPPC:DPPG along with  $\sim 20\text{ wt } \%$  dSP-C was prepared by mixing the appropriate amounts of the phospholipid stock solution together with an aliquot from the stock solution of dSP-C that had been neutralized to pH  $\sim 7$ . This organic solution was placed on a  $\text{CaF}_2$  disk and the solvent allowed to dry, similar to the samples in Figs. 3 and 5. The result is shown in the upper spectrum (A) of Fig. 6. Two major bands are seen in this spectrum, one at  $\sim 1740$

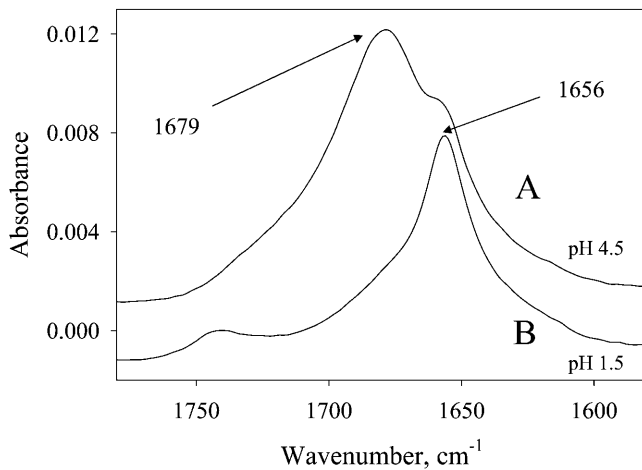


FIGURE 5 Transmission IR spectra of dSP-C in the amide I spectral region. Samples were prepared by titration of stock dSP-C sample (dissolved in 7:1 MeOH:CHCl<sub>3</sub> + 5% 0.1 N HCl). The sample was first titrated to neutral pH with 0.01 N NaOH, followed by reverse titration to acid pH values with 0.01 N HCl. Aliquots were obtained at the pH values indicated in the figure and placed on CaF<sub>2</sub> windows. Spectra were obtained after solvent evaporation. (A) Upper spectrum. Sample obtained at pH 4.5. (B) Lower spectrum. Sample obtained at pH 1.5.

cm<sup>-1</sup> due to the lipid carbonyl groups, and one at 1682 cm<sup>-1</sup> due to the  $\beta$ -sheet structure. Clearly, dSP-C at neutral pH retains its amyloid fibril conformation when co-deposited from organic solution as a mixed lipid-protein complex.

Aqueous multilamellar lipid-protein vesicles of DPPC:DPPG/dSP-C were also formed by drying the co-solubilized lipid-protein organic solution in an N<sub>2</sub> stream, after which the lipid-protein film was rehydrated, followed

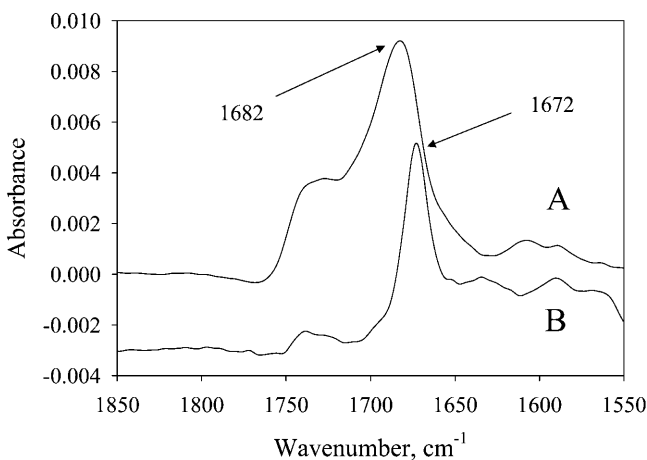


FIGURE 6 Transmission IR spectra of dSP-C in the amide I spectral region. Samples were prepared as lipid-protein complexes by co-solubilization in CHCl<sub>3</sub>:MeOH of DPPC:DPPG (7:3) with 20 wt % dSP-C. Before mixture with lipids, dSP-C was first adjusted to neutral pH. (A) Upper spectrum. Lipid-protein complex co-deposited from organic solution on CaF<sub>2</sub> disk. Spectrum obtained after solvent evaporation. (B) Lower spectrum. Multilamellar lipid-protein vesicles prepared from D<sub>2</sub>O solution. Spectrum obtained using a 20- $\mu$ m pathlength cell with CaF<sub>2</sub> windows.

by several cycles of heating and cooling above the lipid  $T_m$ . D<sub>2</sub>O was used as the rehydration solvent rather than H<sub>2</sub>O to avoid interference from the large  $\delta$ (H-O-H) deformation vibration at  $\sim$ 1640 cm<sup>-1</sup> that hinders quantitative subtracting of the H<sub>2</sub>O background and complicates the analysis of the protein amide I vibration (Parker, 1983). The use of D<sub>2</sub>O results in a  $\delta$ (D-O-D) deformation vibration in a region separate from the amide I vibration, but it also results in a slight shift of the protein amide I vibrations to lower wavenumber (termed amide I'), due to H  $\rightarrow$  D exchange. Transmission IR spectroscopy of the aqueous DPPC:DPPG/dSP-C multilayers containing neutral dSP-C was performed using CaF<sub>2</sub> windows and a 6- $\mu$ m pathlength spacer. The results are shown as the lower spectrum (B) in Fig. 6. The main amide I' protein vibration at 1672 cm<sup>-1</sup> indicates that dSP-C has undergone an unknown amount of H  $\rightarrow$  D exchange. However, the presence of a single amide I' peak slightly shifted from the amide I peak of the original lipid-protein film indicates that the amyloid fibril structure of dSP-C is retained when it is incorporated into lipid-protein multilayers in aqueous suspension.

### The dSP-C secondary structure in transferred Langmuir-Blodgett films

In addition to looking at the solution phase structure of dSP-C, we have also obtained the IR attenuated total reflectance (ATR) spectra of lipid-protein monolayers transferred to Ge ATR crystals from the A/W interface via the Langmuir-Blodgett method. Samples for ATR transfer were prepared similarly to the lipid-protein samples used for the solution studies described above (Fig. 6). An organic solution containing 7:3 DPPC:DPPG along with  $\sim$ 10 wt % dSP-C was prepared by mixing the appropriate amounts of the phospholipid stock solution together with an aliquot from the stock solution of dSP-C that had been neutralized to pH  $\sim$ 7. Fig. 7 illustrates the transmission IR spectrum of the DPPC:DPPG/dSP-C spreading solution used for L-B film transfer. In this figure, the lipid-protein organic solution was placed on a CaF<sub>2</sub> disk and the solvent allowed to dry before acquiring the IR spectrum, similar to the samples in Figs. 3 and 5. The single amide I vibration at 1680 cm<sup>-1</sup> indicates that dSP-C is in the amyloid  $\beta$ -structure conformation in the spreading solution.

An aliquot from the 10 wt % DPPC:DPPG/dSP-C spreading solution was placed at the A/W interface of a LB film balance. The monomolecular film was compressed to the desired surface pressure and subsequently transferred to Ge ATR crystals as described in the Materials and Methods section. The resulting ATR-IR spectra of the 10 wt % PC:PG/dSP-C sample transferred at 30, 45, and 60 mN/m are shown in Fig. 8 A.

It is immediately clear from Fig. 8 A that the IR spectrum of the amide I region of the transferred L-B film of 10 wt %

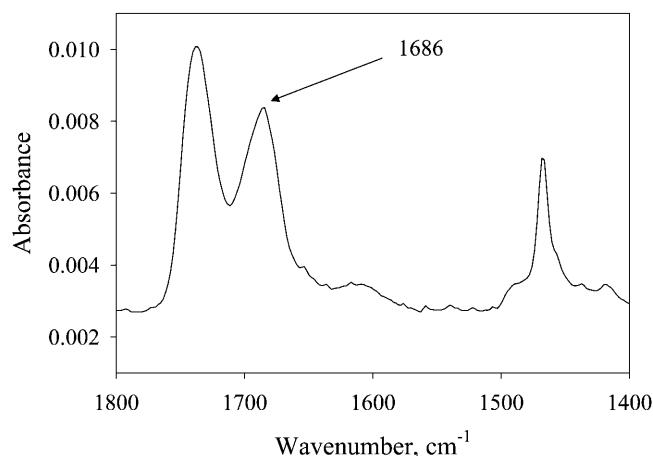


FIGURE 7 Transmission IR spectroscopy of lipid-protein spreading solution used for Langmuir-Blodgett transfers. The solution was prepared by co-solubilization of DPPC:DPPG (7:3) in  $\text{CHCl}_3$ :MeOH (1:1) with 10 wt % dSP-C. Before mixture with lipids, the dSP-C solution was first adjusted to neutral pH. Spectrum was obtained after solvent evaporation.

DPPC:DPPG/dSP-C does not match that of the spreading solution shown in Fig. 7. Two differences are readily apparent. First, the amide I band at  $1680\text{ cm}^{-1}$  corresponding to the amyloid fibril  $\beta$ -strand conformation is absent in the IR spectrum of the L-B film. Instead, a broad amide I band exists that has its maximum peak position at  $\sim 1656\text{ cm}^{-1}$ , indicating an  $\alpha$ -helical secondary structure, albeit one that also has some contribution from  $\beta$ -sheet conformation. In particular, the L-B film transferred at 30 mN/m in Fig. 8 A shows a shoulder at  $\sim 1634\text{ cm}^{-1}$  as well as a broad underlying IR intensity in the range of  $1660\text{--}1690\text{ cm}^{-1}$ . Both these spectral features indicate the involvement of  $\beta$ -structure in the transferred film.

The second difference between the IR spectra of the DPPC:DPPG/dSP-C lipid-protein complex in solution and in L-B transferred films is the fact that dSP-C is not membrane-associated at higher surface pressures. It is obvious from Fig. 8 A that increasing the surface pressure results in a progressive dissociation of 10 wt % dSP-C from the monolayer film, with all of the protein being lost from the surface by 60 mN/m. In fact, an examination of the integrated intensities of the protein amide vibration versus the lipid carbonyl band shows that even at 30 mN/m, dSP-C has been partially desorbed from the surface. In Fig. 7, the ratio of the integrated intensity of the

$$\frac{I_{\text{protein}}}{I_{\text{lipid}}}$$

protein amide I vibration to that of the lipid carbonyl in the spreading solution equals 0.74. In Fig. 8 A, this same ratio is 0.53 for the L-B film transferred at 30 mN/m, 0.28 for the L-B film transferred at 45 mN/m, and 0 for the L-B film transferred at 60 mN/m.

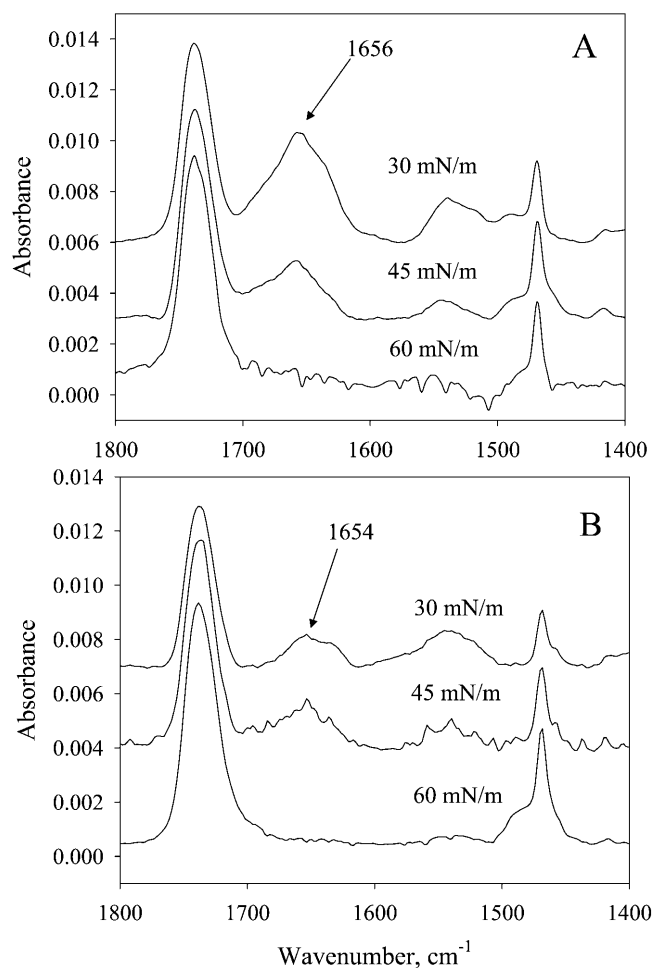


FIGURE 8 Attenuated total reflectance IR spectra of Langmuir-Blodgett monolayer films transferred to Ge ATR crystals. Samples were prepared as lipid-protein complexes by co-solubilization in  $\text{CHCl}_3$ :MeOH of DPPC:DPPG (7:3) with a dSP-C solution that was first adjusted to neutral pH. The monomolecular film was transferred to the Ge crystal at the indicated surface pressures. ATR-IR spectra of transferred monolayer film of (A) DPPC:DPPG (7:3) plus 10 wt % dSP-C and (B) DPPC:DPPG (7:3) plus 5 wt % dSP-C.

The same situation holds for other DPPC:DPPG/dSP-C samples prepared at different lipid-protein ratios. Fig. 8 B presents the ATR-IR spectra of L-B monolayers containing 7:3 DPPC:DPPG plus 5 wt % dSP-C transferred at different surface pressures. The DPPC:DPPG/dSP-C sample with 5 wt % dSP-C (Fig. 8 B) behaves identically to the DPPC:DPPG/dSP-C sample containing 10 wt % dSP-C (Fig. 8 A). That is, 5 wt % dSP-C is progressively excluded from the lipid monolayer as the surface pressure increases (30 and 45 mN/m), and is completely absent from the membrane interface when the surface pressure reaches 60 mN/m.

Several possible explanations may account for the differences between the solution IR spectra of dSP-C (Figs. 3–7) and the interfacial IR spectra of the same protein (Fig. 8). First, the absence of amyloid  $\beta$ -structure at the A/W interface

is likely due to the solubility of smaller dSP-C oligomers. It has been postulated that the formation of insoluble fibril plaques of dSP-C proceeds through the intermediate formation of smaller, soluble aggregates (Johansson, 2001). A previous study using electrospray ionization mass spectrometry indicated that centrifugation at  $20,000 \times g$  was needed to pellet larger dSP-C fibrils, whereas prefibrillar aggregates or oligomers of dSP-C remained soluble in solution (Gustafsson et al., 2001). The lack of a large aggregation band at  $\sim 1620 \text{ cm}^{-1}$  suggests that we do not have large, higher-order, insoluble, aggregated plaques of dSP-C present in our samples. It is therefore quite likely that smaller dSP-C  $\beta$ -strands, whose presence is indicated by the  $1680 \text{ cm}^{-1}$  band in solution, would be soluble and not surface-associated.

Secondly, the ATR-IR spectra of the transferred films seen in Fig. 8 may be explained by the residual helical forms of dSP-C. A previous study reported that delipidation of SP-C reduces, but does not eliminate, the helical content of the deacylated protein (Johansson et al., 1995). This is also the behavior that we observe in the pH-dependent IR transmission spectra of dSP-C, where at neutral pH, the residual  $\alpha$ -helical content of the protein is  $\sim 30\%$  (Figs. 3 and 4).

While deacylation of SP-C results in a coexistence of  $\alpha$  and  $\beta$  structures, we find that it is the helical form of dSP-C that remains membrane associated at the A/W interface, likely due to the hydrophobic alignment of the protein's  $\alpha$ -helix with the hydrocarbon chains of the surrounding phospholipid molecules. However, probably due to the absence of the palmitoyl chains that serve to anchor acylated SP-C to the membrane, increasing surface pressure is sufficient to exclude the deacylated  $\alpha$ -helical dSP-C from the membrane interface (Fig. 8). It is also possible that increasing lateral surface pressure drives dSP-C from a metastable  $\alpha$ -helical into a  $\beta$ -strand conformation, thereby increasing the solubility of the protein and eliminating it from the membrane surface. However, we have not been able to experimentally confirm this.

A previous reflectance IR study of deacylated SP-C at the A/W interface showed no change in secondary structure between deacylated and dipalmitoylated SP-C (Flach et al., 1999). These authors found that the  $\alpha$ -helix secondary structure and tilt angle of SP-C remain unaffected by deacylation. In fact, our current results are not inconsistent with the conclusions of that study. The previous study only examined the IR spectra of deacylated SP-C in a DPPC monolayer at one surface pressure,  $\sim 28 \text{ mN/m}$ . As seen in Fig. 8, our ATR-IR spectra of 10 wt % dSP-C in a lipid monolayer at  $\sim 30 \text{ mN/m}$  (Fig. 8 A) would also be consistent with an interpretation of a primarily helical protein at the A/W interface. Only further examination of dSP-C at additional surface pressures and in additional environments revealed 1), the presence of a unique  $\beta$ -structure for the deacylated, amyloid form of this protein; and 2), that dSP-C is excluded from the membrane surface at high surface pressures.

## The dSP-C secondary structure at the A/W interface

We have also used polarization-modulation infrared reflectance spectroscopy (PM-IRRAS) to study the structure of dSP-C and DPPC:DPPG/dSP-C monolayers in situ at the A/W interface. PM-IRRAS has several advantages over conventional polarized IR reflectance spectroscopy for the study of monolayer films at the A/W interface, specifically the ability to discriminate against isotropic water and water vapor absorptions, and the ability to analyze the resulting spectra directly for the orientation and conformation of the interfacial monolayer (Blaudez et al., 1996). However, PM-IRRAS does have potential shortcomings when applied to monomolecular films. Because PM-IRRAS is based on the rapid modulation of polarized electromagnetic radiation reflected from the interface, one disadvantage of the technique is that the absence of a signal does not necessarily indicate the absence of a monolayer at the surface. Rather, the absence of a signal could indicate either an isotropic monomolecular film or a preferred monolayer orientation in which the transition dipole moment is oriented such that co-existing positive and negative signal contributions cancel one another (Blaudez et al., 1996). Therefore, interpretation of PM-IRRAS spectra is best accomplished in conjunction with other information.

Fig. 9 illustrates the amide I and amide II regions in PM-IRRAS spectra of dSP-C protein monolayers at the A/W interface acquired at different surface pressures. In the spectra shown in Fig. 9 A, the dSP-C protein was applied to the A/W interface at low surface pressure as an acidic solution of pH 1.8; spectra were acquired during compression of the monolayer to higher surface pressures. The subphase was 120 mM NaCl adjusted to pH 7. The most prominent band in this spectrum is the amide I vibration at  $1656 \text{ cm}^{-1}$ . As previously described, this wavenumber position corresponds to an  $\alpha$ -helical conformation for the dSP-C monolayer, which also corresponds to the structure of dSP-C in solution at low pH (Fig. 3). According to the PM-IRRAS "surface selection rule," strong positive bands in PM-IRRAS spectra indicate that the corresponding transition dipole moments are preferentially oriented in the plane of the surface (Blaudez et al., 1996). If we assume that the protein's  $\alpha$ -helix lies along the water surface, then (depending upon the choice made for the angle between the amide I transition moment and the long axis of the  $\alpha$ -helix; see, e.g., Buffeteau et al., 2000), this implies that the dSP-C  $\alpha$ -helix is oriented at a maximum angle of  $29\text{--}38^\circ$  from the interface.

Fig. 9 B presents PM-IRRAS spectra for dSP-C protein monolayers in which the dSP-C spreading solution was first neutralized to pH 7 before spreading at the A/W interface. Surprisingly, the PM-IRRAS spectra of a dSP-C monolayer spread from a neutral solution are indistinguishable from that of the dSP-C monolayer in acid form (Fig. 9 A), even though the same neutral dSP-C solution produced a transmission IR spectrum of a  $\beta$ -strand (Fig. 3).

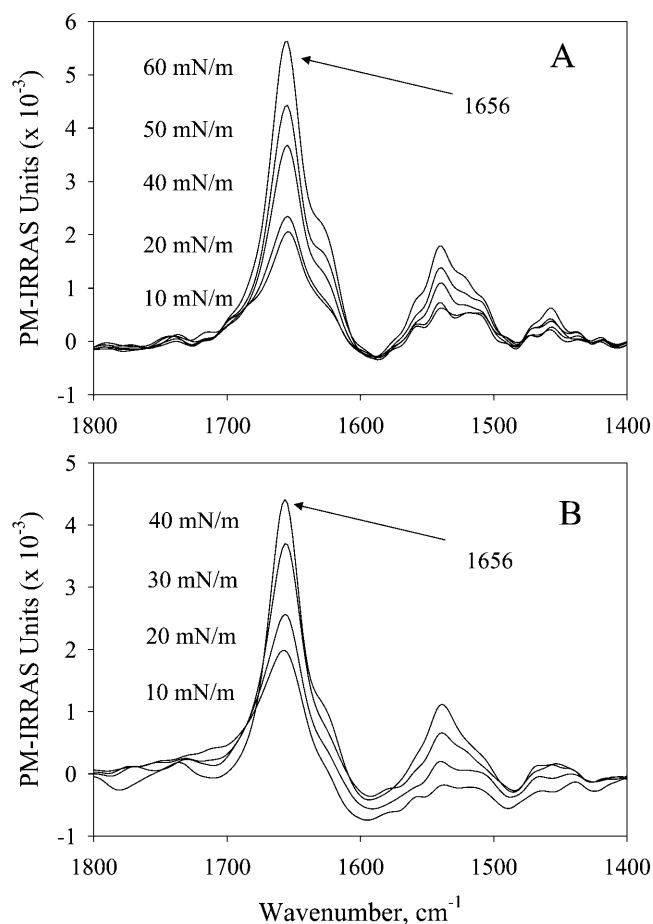


FIGURE 9 PM-IRRAS spectra of dSP-C protein monolayers at the A/W interface. The dSP-C protein was applied in organic solution to the A/W interface at low surface pressure. Spectra were acquired at the indicated surface pressures during compression of the monolayer. The subphase was 120 mM NaCl adjusted to pH 7. (A) Spectra of dSP-C with spreading solution adjusted to pH 1.8. (B) Spectra of dSP-C with spreading solution adjusted to pH 7.

The helix-like PM-IRRAS spectra of a neutral dSP-C monolayer seen in Fig. 9 B are explainable if one assumes that the interfacial pH is significantly more acidic than the subphase pH. This may, in fact, be the case. Many previous surface chemistry publications have postulated that the pH of the water surface should be different than the bulk pH of the water subphase, although direct proof of such a difference is difficult to obtain; see, e.g., references cited in Le Calvez et al. (2001). Two recent vibrational spectroscopy articles have offered new data to suggest that a  $\Delta$ pH between bulk and interface does exist and that this pH difference depends upon the counterions present in solution (Miranda et al., 1998; Le Calvez et al., 2001). Using PM-IRRAS and sum frequency generation of fatty acid monolayers at the A/W interface, it was shown that the pH dependence of the acid dissociation reaction is strongly influenced by the subphase counterion. Specifically, with  $\text{Na}^+$  ions, deprotonation of the fatty acid was very difficult to achieve, and required a pH of

$\sim 10$  for half-neutralization of the fatty acid. This is 3–4 pH units greater than was the case with ions such as  $\text{Cd}^{2+}$  or  $\text{Ca}^{2+}$  and leads to an estimate that the  $\text{H}_3\text{O}^+$  concentration at the interface could be on the order of 1000–10,000 times greater than in the bulk (Le Calvez et al., 2001). Given the very sensitive pH dependence of the metastable  $\alpha$ -helix  $\rightarrow$   $\beta$ -strand  $\rightarrow$   $\alpha$ -helix transition for dSP-C in solution that we demonstrated in Figs. 3 and 5, it is possible that a highly acidic interfacial pH caused a conformational rearrangement of the neutral dSP-C from the  $\beta$ -strand  $\rightarrow$   $\alpha$ -helix form. If this can be confirmed, this would suggest a potential mechanism for the formation of amyloid SP-C fibrils at the alveolar interface in disease states such as PAP.

We have also used PM-IRRAS to investigate the structure of DPPC:DPPG/dSP-C lipid-protein monolayers at the A/W interface. Samples for study at the A/W interface were prepared identically to the lipid-protein samples described above for the solution studies (Fig. 6) and ATR transfer studies (Fig. 8). Fig. 10 presents PM-IRRAS spectra for two types of lipid protein monolayers. Fig. 10 A shows the spectra of 10 wt % DPPC/DPPG/dSP-C in which the dSP-C stock solution was pH 1.8, whereas Fig. 10 B shows the spectra of 10 wt % DPPC/DPPG/dSP-C monolayers in which the dSP-C stock solution was first adjusted to pH 7 before preparing the sample. In Fig. 10, a PM-IRRAS spectrum is presented for both types of lipid-protein monolayers at a low surface pressure ( $\sim 5$  mN/m) and at a high surface pressure ( $\sim 40$  mN/m).

As seen in both Fig. 10, A and B, the most prominent peak in the PM-IRRAS spectra of DPPC/DPPG/dSP-C monolayers is the lipid carbonyl band at  $\sim 1740$   $\text{cm}^{-1}$ . The strong downward sloping baseline between 1700 and 1650  $\text{cm}^{-1}$  is due to the anomalous dispersion of the real part of the refractive index of water in this region, arising from the  $\delta$  (H-O-H) deformation vibration of liquid water (Blaudez et al., 1996).

The most noticeable aspect of the amide I vibrations in the range 1700–1600  $\text{cm}^{-1}$  for both types of DPPC/DPPG/dSP-C monolayers is the fact that they are extremely weak or nonexistent. At low surface pressures ( $\sim 5$  mN/m), small positive PM-IRRAS signals in the range 1670–1660  $\text{cm}^{-1}$  indicate a small amount of  $\beta$ -strand structure is present, as was also noticed in the ATR-transferred films for these monolayers (Fig. 8). However, no dominant amide I vibration due to an  $\alpha$ -helix conformation is seen in these spectra at either low or high surface pressures.

The most likely explanation for the absence of PM-IRRAS bands due to the  $\alpha$ -helix in these spectra is that no preferential orientation exists for the helix fraction of dSP-C. While a defined orientation has been established for the fully acylated form of SP-C (Gericke et al., 1997), we have shown that 1), dSP-C in lipid-protein monolayers exists as a mixture of soluble  $\beta$ -strand and membrane-associated  $\alpha$ -helix conformations; and 2), that the membrane-associated  $\alpha$ -helix dissociates from the membrane or enters the

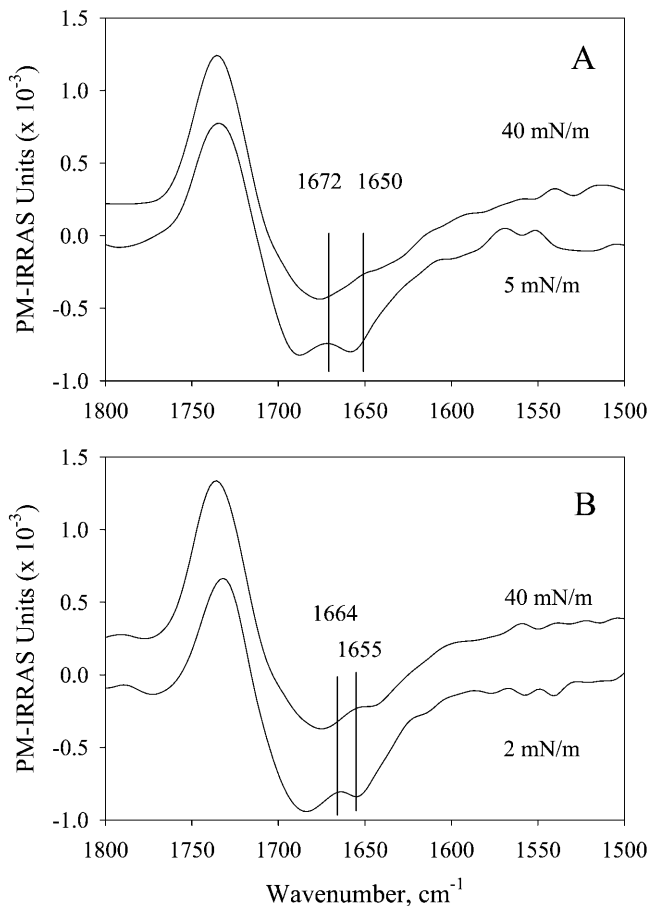


FIGURE 10 PM-IRRAS spectra of dSP-C lipid-protein monolayers at the A/W interface. The monolayer was applied in organic solution to the A/W interface at low surface pressure. Spectra were acquired at the indicated surface pressures during compression of the monolayer. The lipid-protein film used was DPPC:DPPG (7:3) plus 10 wt % dSP-C. The subphase was 120 mM NaCl adjusted to pH 7. (A) Spectra of DPPC/DPPG/dSP-C with dSP-C spreading solution adjusted to pH 1.8. (B) Spectra of DPPC/DPPG/dSP-C with dSP-C spreading solution adjusted to pH 7.

subphase as a function of applied surface pressure. Since dSP-C readily dissociates from the interface (unlike fully acylated SP-C), it is unlikely to have a defined orientation in its membrane-associated form. A random or isotropic orientation of dSP-C would not produce a detectable PM-IRRAS signal.

## CONCLUSIONS

We employed IR spectroscopy to study the pH dependence of the conformation of deacylated SP-C (dSP-C), which was observed to aggregate and form amyloid fibrils in solution. Several different IR techniques were used to study the structure of dSP-C in various environments: 1), transmission IR spectroscopy was used to study the conformation of dSP-C in solutions and bulk liposomes; 2), attenuated total reflectance (ATR) spectroscopy was used to study the

structure of dSP-C in monomolecular films transferred onto solid substrates; and 3), photoelastic modulation IR reflection absorption spectroscopy (PM-IRRAS) was used to study the structure of dSP-C monolayers in situ at the A/W interface. This work identified pH as a specific cause of conformational changes in dSP-C, and a possible contributor to amyloid fibril formation in pulmonary alveolar proteinosis. Our detailed conclusions are as follows.

The formation of amyloid fibrils from dSP-C may be observed in solution using visible light microscopy. The visible images of the fibrils produced from dSP-C isolated in our laboratory are consistent with previously published images of amyloid fibrils isolated from the bronchoalveolar lavage of a clinical patient suffering from pulmonary alveolar proteinosis (PAP) and attributed to deacylated SP-C. Mass spectrometry (MALDI-TOF) confirmed that the dSP-C protein used in these experiments was in the deacylated forms.

Solution phase IR spectra of dSP-C demonstrated that the deacylated protein at low pH primarily adopts an  $\alpha$ -helical secondary structure similar to that of the fully acylated protein at neutral pH. However, as the pH is raised, an  $\alpha$ -helix  $\rightarrow$   $\beta$ -strand conformational change occurs in dSP-C. The IR spectrum of dSP-C at neutral pH is consistent with a main conformation of short segments of twisted or coiled  $\beta$ -sheet strands or  $\beta$ -hairpins in an amyloid fibril structure. Deacylation of SP-C reduced, but did not eliminate, the helical content of the deacylated protein; residual  $\alpha$ -helix structure was also present in dSP-C at neutral pH. The full  $\alpha$ -helix structure of dSP-C is recoverable from the amyloid  $\beta$ -structure when the pH is lowered. When mixed with lipids in solution, dSP-C at neutral pH retains its amyloid fibril  $\beta$ -strand conformation when deposited from organic solution as a lipid-protein complex. In addition, the amyloid fibril structure of dSP-C is retained when it is incorporated into lipid-protein multilayers in aqueous solution.

ATR-IR spectra of Langmuir-Blodgett monolayer films transferred to solid substrates demonstrated that the amyloid fibril  $\beta$ -strand conformation was absent in the IR spectrum of the L-B film. The absence of amyloid  $\beta$ -structure at the A/W interface and in the L-B monolayers is likely due to the solubility of smaller dSP-C oligomers. A broad amide I contour centered at  $1656\text{ cm}^{-1}$  indicated that an  $\alpha$ -helical secondary structure was the primary conformation present in the L-B transferred films. However, the residual dSP-C  $\alpha$ -helix was not strongly membrane-associated, as increasing the monolayer lateral surface pressure to 60 mN/m was sufficient to exclude all the remaining protein from the membrane interface.

PM-IRRAS spectra of dSP-C protein monolayers in situ at the A/W interface demonstrated that dSP-C exists as

an  $\alpha$ -helix oriented at a maximum of 29–38° from the interface when spread from a pH-adjusted, neutral solution, even though the same neutral dSP-C solution produced a transmission IR spectrum of a  $\beta$ -strand. We established that the dSP-C  $\alpha$ -helix is metastable and pH-sensitive in solution; therefore, it is likely that a surface-specific mechanism caused a conformational rearrangement of the neutral dSP-C from the  $\beta$ -strand  $\rightarrow$   $\alpha$ -helix form. The most probable explanation is that an increased concentration of  $\text{H}_3\text{O}^+$  ion exists at the A/W interface and contributes to an effective low interfacial pH. If this can be confirmed, this would suggest a potential mechanism for the formation of amyloid SP-C fibrils at the alveolar interface in disease states such as PAP. PM-IRRAS was also used to study lipid-protein monolayers containing dSP-C in situ at the A/W interface, but showed no discernable amide I band that could be attributed to an  $\alpha$ -helix, suggesting that the residual dSP-C helix conformation seen in the ATR-IR spectra of transferred films is randomly or isotropically oriented before exclusion from the membrane interface.

We thank Dr. Dennis Phillips of the Chemical and Biological Mass Spectrometry Facility at the University of Georgia for his help with the MALDI-TOF studies of dSP-C.

The work described here was supported by the U.S. Public Health Service through National Institutes of Health grants EB001956 (to R.A.D.) and HL66066 (to J.E.B.).

## REFERENCES

- Amrein, M., A. von Nahmen, and M. Sieber. 1997. A scanning force and fluorescence light microscopy study of the structure and function of a model pulmonary surfactant. *Eur. Biophys. J.* 26:349–357.
- Avery, M. E., and J. Mead. 1959. Surface properties in relation to atelectasis and hyaline membrane disease. *Am. J. Dis. Child.* 97:517–523.
- Baatz, J. E., Y. Zou, J. T. Cox, Z. Wang, and R. H. Notter. 2001. High yield purification of lung surfactant proteins SP-B and SP-C and the effects on surface activity. *Prot. Express. Purificat.* 23:180–190.
- Bi, X., C. Flach, J. Perez-Gil, I. Plasencia, D. Andreu, E. Oliveira, and R. Mendelsohn. 2002. Secondary structure and lipid interactions of the N-terminal segment of pulmonary surfactant SP-C in Langmuir films: IR reflection-absorption spectroscopy and surface pressure studies. *Biochemistry.* 41:8385–8395.
- Blaudez, D., T. Buffeteau, J. C. Cornut, B. Desbat, N. Escafre, M. Pezolet, and J. M. Turllet. 1993. Polarization-modulated FT-IR spectroscopy of a spread monolayer at the air/water interface. *Appl. Spectrosc.* 47:869–874.
- Blaudez, D., J.-M. Turllet, J. Dufourcq, D. Bard, T. Buffeteau, and B. Desbat. 1996. Investigations at the air/water interface using polarization modulation IR spectroscopy. *J. Chem. Soc. Faraday Trans.* 92:525–530.
- Brockman, J. M., Z. Wang, R. H. Notter, and R. A. Dluhy. 2003. Effect of hydrophobic surfactant proteins SP-B and SP-C on binary phospholipid monolayers. II. Infrared external reflectance-absorption spectroscopy. *Biophys. J.* 84:326–340.
- Buffeteau, T., B. Desbat, M. Pezolet, and J. M. Turllet. 1993. Orientational studies of polymers using polarization modulation IR linear dichroism: experimental procedure and quantitative analysis. *J. Chim. Phys. Phys.-Chim. Biol.* 90:1467–1489.
- Buffeteau, T., E. Le Calvez, S. Castano, B. Desbat, D. Blaudez, and J. Dufourcq. 2000. Anisotropic optical constants of  $\alpha$ -helix and  $\beta$ -sheet secondary structures in the infrared. *J. Phys. Chem. B.* 104:4537–4544.
- Buffeteau, T., and M. Pezolet. 1996. In situ study of photoinduced orientation in azopolymers by time-dependent polarization modulation infrared spectroscopy. *Appl. Spectrosc.* 50:948–955.
- Cameron, D. G., J. K. Kauppinen, and D. Moffatt. 1982. Precision in condensed phase vibrational spectroscopy. *Appl. Spectrosc.* 36:245–250.
- Creuwels, L. A. J. M., L. M. G. van Golde, and H. P. Haagsman. 1997. The pulmonary surfactant system: biochemical and clinical aspects. *Lung.* 175:1–39.
- Dluhy, R. A. 2000. Infrared spectroscopy of biophysical monolayer films at interfaces. Theory and applications. In *Physical Chemistry of Biological Interfaces*. A. Baszkin, and W. Norde, editors. Marcel Dekker, New York. 711–747.
- Dluhy, R. A., K. E. Reilly, R. D. Hunt, M. L. Mitchell, A. J. Mautone, and R. Mendelsohn. 1989. Infrared spectroscopic investigations of pulmonary surfactant. Surface film transitions at the air-water interface and bulk phase thermotropism. *Biophys. J.* 56:1173–1181.
- Flach, C. R., A. Gericke, K. M. W. Keough, and R. Mendelsohn. 1999. Palmitoylation of lung surfactant protein SP-C alters surface thermodynamics, but not protein secondary structure or orientation in 1,2-dipalmitoylphosphatidylcholine Langmuir films. *Biochim. Biophys. Acta.* 1416:11–20.
- Galla, H. J., N. Bourdos, A. von Nahmen, M. Amrein, and M. Sieber. 1998. The role of pulmonary surfactant protein C during the breathing cycle. *Thin Solid Films.* 329:632–635.
- Gericke, A., C. R. Flach, and R. Mendelsohn. 1997. Structure and orientation of lung surfactant SP-C and L- $\alpha$ -dipalmitoylphosphatidylcholine in aqueous monolayers. *Biophys. J.* 73:492–499.
- Goormaghtigh, E., V. Cabiaux, and J.-M. Ruyschaert. 1994. Determination of soluble and membrane protein structure by Fourier transform infrared spectroscopy. I. Assignments and model compounds. In *Physicochemical Methods in the Study of Biomembranes*. H. J. Hilderson, and G. B. Ralston, editors. Plenum Press, New York. 329–362.
- Gustafsson, M., W. Griffiths, E. Furujo, and J. Johansson. 2001. The palmitoyl groups of lung surfactant protein C reduce unfolding into a fibrillogenic intermediate. *J. Mol. Biol.* 310:937–950.
- Gustafsson, M., J. Thyberg, J. Näslund, E. Eliasson, and J. Johansson. 1999. Amyloid fibril formation by pulmonary surfactant protein C. *FEBS Lett.* 464:138–142.
- Harris, P. I. 2000. Fourier transform infrared spectroscopic studies of peptides: potentials and pitfalls. In *Infrared Analysis of Peptides and Proteins: Principles and Applications*. B. Ram Singh, editor. American Chemical Society, Washington, DC. 54–95.
- Hawgood, S., and K. Schiffer. 1991. Structures and properties of the surfactant-associated proteins. *Annu. Rev. Physiol.* 53:375–394.
- Holm, B. A., Z. Wang, E. A. Egan, and R. H. Notter. 1996. Content of dipalmitoyl phosphatidylcholine in lung surfactant: ramifications for surface activity. *Pediatr. Res.* 39:805–811.
- Hunt, A. N., F. J. Kelly, and A. D. Postle. 1991. Developmental variation in whole human lung phosphatidylcholine molecular species: a comparison of guinea pig and rat. *Early Hum. Dev.* 25:157–171.
- Jackson, M., and H. H. Mantsch. 1993. Biomembrane structure from FT-IR spectroscopy. *Spectrochim. Acta Rev.* 15:53–69.
- Johansson, J. 2001. Membrane properties and amyloid fibril formation of lung surfactant protein C. *Biochem. Soc. Trans.* 29:601–606.
- Johansson, J., T. Curstedt, and B. Robertson. 1994a. The proteins of the surfactant system. *Eur. Respir. J.* 7:372–391.
- Johansson, J., G. Nilsson, R. Stromberg, B. Robertson, H. Jornvall, and T. Curstedt. 1995. Secondary structure and biophysical activity of synthetic analogues of the pulmonary surfactant polypeptide SP-C. *Biochem. J.* 307:535–541.

- Johansson, J., T. Szyperski, T. Curstedt, and K. Wüthrich. 1994b. The NMR structure of the pulmonary surfactant-associated polypeptide SP-C in an apolar solvent contains a valyl-rich  $\alpha$ -helix. *Biochemistry*. 33:6015–6023.
- Kahn, M. C., G. J. Anderson, W. R. Anyan, and S. B. Hall. 1995. Phosphatidylcholine molecular species of calf lung surfactant. *Am. J. Physiol.* 13:L567–L573.
- Kallberg, Y., M. Gustafsson, B. Persson, J. Thyberg, and J. Johansson. 2001. Prediction of amyloid fibril-forming proteins. *J. Biol. Chem.* 276:12945–12950.
- Koppaka, V., and P. H. Axelsen. 2000. Accelerated accumulation of amyloid beta proteins on oxidatively damaged lipid membranes. *Biochemistry*. 39:10011–10016.
- Kramer, A., A. Wintergalen, M. Sieber, H. J. Galla, M. Amrein, and R. Guckenberger. 2000. Distribution of the surfactant-associated protein C within a lung surfactant model film investigated by near-field optical microscopy. *Biophys. J.* 78:458–465.
- Krimm, S., and J. Bandekar. 1986. Vibrational spectroscopy and conformation of peptides, polypeptides, and proteins. *Adv. Prot. Chem.* 38:181–364.
- Krüger, P., J. E. Baatz, R. A. Dluhy, and M. Lösche. 2002. Effect of the hydrophobic peptide SP-C on binary phospholipid monolayers. Molecular machinery at the air/water interface. *Biophys. Chem.* 99:209–228.
- Krüger, P., M. Schalke, Z. Wang, R. H. Notter, R. A. Dluhy, and M. Lösche. 1999. Effect of hydrophobic surfactant peptides SP-B and SP-C on binary phospholipid monolayers. I. Fluorescence and dark-field microscopy. *Biophys. J.* 77:903–914.
- Kubelka, J., and T. A. Keiderling. 2001a. The anomalous infrared amide I intensity distribution in  $^{13}\text{C}$  isotopically labelled peptide  $\beta$ -sheets comes from extended, multiple-stranded structures. An ab initio study. *J. Am. Chem. Soc.* 123:6142–6150.
- Kubelka, J., and T. A. Keiderling. 2001b. Differentiation of  $\beta$ -sheet forming structures: ab initio-based simulations of IR absorption and vibrational CD for model and protein  $\beta$ -sheets. *J. Am. Chem. Soc.* 123:12048–12058.
- Le Calvez, E., D. Blaudez, T. Buffeteau, and B. Desbat. 2001. Effect of cations on the dissociation of arachidonic acid monolayers on water studied by polarization-modulated infrared reflection-absorption spectroscopy. *Langmuir*. 17:670–674.
- Lewis, J. F., and A. H. Jobe. 1993. Surfactant and the adult respiratory distress syndrome. *Am. Rev. Respir. Dis.* 147:218–233.
- Mendelsohn, R., J. W. Brauner, and A. Gericke. 1995. External infrared reflection-absorption spectrometry. Monolayer films at the air-water interface. *Annu. Rev. Phys. Chem.* 46:305–334.
- Miranda, P. B., Q. Du, and Y. R. Shen. 1998. Interaction of water with a fatty acid Langmuir film. *Chem. Phys. Lett.* 286:1–8.
- Morrissey, J. H. 1981. Silver stain for proteins in polyacrylamide gels: a modified procedure with enhanced uniform sensitivity. *Anal. Biochem.* 117:307–310.
- Notter, R. H. 2000. Lung Surfactants: Basic Science and Clinical Applications. Marcel Dekker, New York.
- Notter, R. H., and Z. Wang. 1997. Pulmonary surfactant: physical chemistry, physiology and replacement. *Rev. Chem. Eng.* 13:1–118.
- Parker, F. S. 1983. Applications of Infrared, Raman, and Resonance Raman Spectroscopy in Biochemistry. Plenum Press, New York.
- Pastrana-Rios, B., S. Taneva, K. M. W. Keough, A. J. Mautone, and R. Mendelsohn. 1995. External reflection absorption infrared spectroscopy study of lung surfactant proteins SP-B and SP-C in phospholipid monolayers at the air/water interface. *Biophys. J.* 69:2531–2540.
- Pison, U., W. Seeger, R. Buchhorn, T. Joka, M. Brand, U. Obertacke, H. Neuhof, and K. P. Schmit-Nauerburg. 1989. Surfactant abnormalities in patients with respiratory failure after multiple trauma. *Am. Rev. Respir. Dis.* 140:1033–1039.
- Seymour, J. F., and J. J. Presneill. 2002. Pulmonary alveolar proteinosis. Progress in the first 44 years. *Am. J. Respir. Crit. Care Med.* 166:215–235.
- Shanmukh, S., P. Howell, J. E. Baatz, and R. A. Dluhy. 2002. Effect of hydrophobic surfactant proteins SP-B and SP-C on phospholipid monolayers. Protein structure studied using 2D IR and  $\beta\nu$  correlation analysis. *Biophys. J.* 83:2126–2141.
- Shin, Y. S. 1962. Spectrophotometric ultramicrodetermination of inorganic phosphorus and lipid phosphorus in serum. *Anal. Chem.* 34:1164–1166.
- Silva, R. A. G. D., S. A. Sherman, F. Perini, E. Bedows, and T. A. Keiderling. 2000. Folding studies on the human chorionic gonadotropin  $\beta$ -subunit using optical spectroscopy of peptide fragments. *J. Am. Chem. Soc.* 122:8623–8630.
- Szyperski, T., G. Vandenbussche, T. Curstedt, J. M. Ruysschaert, K. Wüthrich, and J. Johansson. 1998. Pulmonary surfactant-associated polypeptide C in a mixed organic solvent transforms from a monomeric  $\alpha$ -helical state into insoluble  $\beta$ -sheet aggregates. *Protein Sci.* 7:2533–2540.
- Vandenbussche, G., A. Clerx, T. Curstedt, J. Johansson, and H. Jornvall. 1992. Structure and orientation of the surfactant-associated protein C in a lipid bilayer. *Eur. J. Biochem.* 203:201–209.
- von Nahmen, A., M. Schenk, M. Sieber, and M. Amrein. 1997. The structure of a model pulmonary surfactant as revealed by scanning force microscopy. *Biophys. J.* 72:463–469.
- Wang, Z., O. Gurel, J. E. Baatz, and R. H. Notter. 1996. Acylation of pulmonary surfactant protein C is required for its optimal surface active interactions with phospholipids. *J. Biol. Chem.* 271:19104–19108.